DOI:10.1021/jf102341r

JOURNAL OF AGRICULTURAL AND FOOD CHEMISTRY
ARTICLE

Nanoemulsions Prepared by a Low-Energy Emulsification Method Applied to Edible Films

Cristina Bilbao-Sáinz,* Roberto J. Avena-Bustillos, Delilah F. Wood, Tina G. Williams, and Tara H. McHugh

Western Regional Research Center, Agricultural Research Service, U.S. Department of Agriculture 800 Buchanan Street, Albany, California 94710, United States

Catastrophic phase inversion (CPI) was used as a low-energy emulsification method to prepare oil-in-water (O/W) nanoemulsions in a lipid (Acetem)/water/nonionic surfactant (Tween 60) system. CPIs in which water-in-oil emulsions (W/O) are transformed into oil-in-water emulsions (O/W) were induced by changes in the phase ratio. Dynamic phase inversion emulsification was achieved by slowly increasing the water volume fraction (f_w) to obtain O/W emulsions from water in oil emulsions. Composition and processing variables were optimized to minimize droplet size and polydispersity index (PdI). It was found that addition of the continuous phase to the dispersed phase following the standard CPI procedure resulted in the formation of oil droplets with diameters of 100−200 nm. Droplet size distribution during CPI and emulsification time depended on stirring speed and surfactant concentration. Droplet sizes in the inverted emulsions were compared to those obtained by direct emulsification: The process time to reach droplet sizes of around 100 nm was reduced by 12 times by using CPI emulsification. The Acetem/water nanoemulsion was also used as a carrier to incorporate oregano and cinnamon essential oils into soy protein edible films. The resulting composite films containing oregano oil showed better moisture barrier and mechanical properties compared to soy protein films.

KEYWORDS: Catastrophic phase inversion; emulsification; nanoemulsion; edible films

INTRODUCTION

Nanoemulsions are a class of emulsions with droplet sizes in the nanometric scale, typically in the range between 50 and 500 nm, although there is no clear agreement in the scientific community on this point. Nanoemulsions may contribute to improve the dispersibility of lipophilic compounds in water and the bioavailability during gastrointestinal passage. In addition, nanoemulsions could be kinetically stable and optically transparent if the system components and preparation method are conveniently selected. Recently, studies have shown the successful application of nanoemulsions in food applications, which include encapsulation of limonene, lutein, and omega-3 fatty acids (*1*, *2*), encapsulation of astaxhantin and lycopene (*2*, *3*), encapsulation of α-tocopherol to reduce lipid oxidation in fish oil (*4*), and the use of nanoemulsions to incorporate essential oils, oleoresins, and oil-based natural flavors into food products such as carbonated beverages and salad dressings (*5*).

Common methods for producing nanoemulsions are high-shear stirring, high-pressure homogenization, or ultrasound generation (*2*, *4*). All of these methods require the input of a considerable amount of mechanical energy. Spontaneous emulsification is a less expensive and energy efficient alternative that takes advantage of the chemical energy stored in the system (*6*).

Spontaneous emulsification involves phase inversions. Phase inversion is the process whereby an oil-in-water system (O/W) inverts into a water-in-oil system (W/O) and vice versa. Spontaneous phase inversions were first reported by Shinoda and co-workers (*7*). Since then, many other scientists have studied spontaneous emulsification (*8*−*12*). There are at least two types of spontaneous emulsification methods: transitional phase inversion and catastrophic phase inversion (CPI). In CPI emulsification, the system usually begins with abnormal emulsions, that is, emulsions in which the surfactant has a high affinity to the dispersed phase. Abnormal emulsions are usually unstable and can only be maintained under vigorous mixing for a short period of time. The ultimate fate of an unstable emulsion is to invert to the opposite state. A CPI is triggered by increasing the rate of droplet coalescence so that the balance between the rate of coalescence and rupture cannot be maintained (*11*). This may be induced by changing the variables that increase the rate of droplet coalescence, such as the continuous addition of dispersed-phase volume, the most common variable used.

One of the difficulties the food industry confronts is that the formation of microemulsions requires >20% more surfactant than typical emulsion formation (*13*). This study evaluates the effects of surfactant concentration on droplet size produced by CPI at different agitation speeds. In addition, the nanoemulsions produced were subsequently used to incorporate essential oils into isolated soybean protein (ISP) composite edible films because soy protein has shown excellent film-forming abilities, producing more flexible, smoother, and clearer films compared to films from other plant protein sources (*14*). The essential oils selected for this

 Published on Web 10/26/2010

Table 1. Film Composition Expressed as Weight Ratios in the Dried ISP-Based Films

film[a]	ISP	glycerol	Acetem	Tween 60	oregano oil	cinnamon oil
ISP	10	4				
AC/ISP	10	4	1	0.5		
OR/AC/ISP	10	4	1	0.5	0.67	
CN/AC/ISP	10	4	1	0.5		0.67

[a] ISP, isolated soybean protein; AC, Acetem; OR, oregano oil; CN, cinnamon oil.

work were cinnamon oil and oregano oil for their flavor and antimicrobial activity. Thus, this work provides useful background information in determining the composition and process parameters for the production of low-cost composite edible films.

MATERIALS AND METHODS

In the experiments described, the nonaqueous phase (oil) was Grindsted Acetem 90-50K kindly provided by Danisco USA Inc. (New Century, KS). This product is an acetic acid ester of monoglycerides made from edible, partially hydrogenated soybean oil. The aqueous phase was purified doubled distilled and filtered (Millipore) water (Barnstead/Thermolyne, Dubuque, IA). The surfactant was polyoxyethylene sorbitan monostearate (Tween 60), which has a hydrophilic−lipophilic balance (HLB) of 14.9 (Sigma-Aldrich Co., Milwaukee, WI).

The target emulsion was an O/W emulsion consisting of Acetem (6 g) in water (30 g) with a weight ratio of 1:5. Weights of 6 g of Acetem and 30 g of purified water were used in all experiments. The surfactant-to-oil weight ratios (S/O) were 0.5, 0.75, and 1.

Direct Emulsification. The surfactant (Tween 60) was mixed in the intended aqueous continuous phase (purified water) for 10 min. The intended dispersed phase (Acetem) was added to the aqueous phase to form an O/W emulsion under agitation. The emulsification process was carried out for 6 h, withdrawing aliquots during this time for droplet size analysis.

The experiments were performed in a 125 mL beaker on a hot plate with temperature control set at 30 °C. A triple-helix conventional mixer (Cole-Parmer Servodyne model 50000-30), connected to a digital variable-speed motor, was used to mix the components. The stirrer speed was set at 700, 1000, and 1300 rpm. Direct and CPI emulsification methods were compared.

CPI Emulsification. CPIs were induced by changes in an emulsion's water-to-oil ratio. Instability of the initial dispersed phase droplets is a requirement of catastrophic inversion. Thus, the hydrophilic surfactant (Tween 60) was placed into the intended dispersed phase (Acetem). The intended continuous phase (purified water) was then added over time to the Acetem/Tween 60 at a rate of 1 mL/min. CPI starts with a W/O emulsion morphology and undergoes inversion to the desired O/W emulsion. After 30 min, when the addition of water was already complete, stirring continued up to an additional 360 min. Sample aliquots were withdrawn during the emulsification process, for droplet size analysis.

Preparation of Isolated Soybean Protein (ISP)-Based Films. ISP with 90% protein on a dry weight basis was supplied by The Solae Co. (San Leandro, CA). Films were plasticized with glycerol from Fisher Scientific Inc. (Pittsburgh, PA). The essential oils (oregano and cinnamon) were purchased from Lhasa Karnak Co. (Berkeley, CA).

Four soy protein-based film formulations (**Table 1**) were prepared and evaluated to demonstrate the effect of Acetem with and without essential oils on water barrier and mechanical properties.

Aqueous solutions of 10% (w/w) ISP were prepared and heated at 90 °C for 45 min in a water bath to denature proteins. Solutions were cooled to room temperature, and glycerol was added to plasticize the films.

O/W emulsions were produced by CPI mixing for 4 h at 700 rpm according to the procedure described above. The emulsions were incorporated into the ISP solution and mixed for an additional 2 h at the same speed. Films containing essential oils were first mixed with the oil phase and vortexed for few seconds to ensure thorough mixing.

The film solutions were degassed under vacuum (up to 1000 mbar) to prevent microbubble formation in the resulting films. Films were cast on glass plates (30 × 30 cm) coated with Mylar (polyester film, DuPont, Hopewell, VA). The emulsions (45 g) were cast to a wet thickness of 1.15 mm onto plates using a metallic casting bar, and the emulsions were allowed to dry at room temperature for 24 h. After drying, the films were removed from the Mylar. Film thicknesses were measured to the nearest 0.001 mm at four positions around the film and in the center using a micrometer. Average values of five thickness measurements per film were used in all water vapor permeability (WVP) calculations.

Droplet Size Measurement. Volume distributions of droplets were measured using a Malvern zetasizer dynamic light scattering particle size analyzer (Malvern Instruments Ltd., Westborough, MA) at 25 °C. The emulsions were first diluted with purified water to $^1/_{10}$ of their original concentrations. Measurements were done in triplicate, and the *z*-average and polydispersity index (PDI) were reported. The *z*-average is a value of the average particle size that the Zetasizer provides by measuring the Brownian motion of the particles and relates it to their size. It does this by illuminating the particles with a laser and analyzing the intensity fluctuations in the scattered light.

Oil droplet size distribution was measured by means of laser light scattering (Horiba LA-900, Ann Arbor, MI) for emulsions with droplet sizes of > 10 μm.

Microscope Analysis. *Light Microscopy*. Emulsions were observed through crossed polarizers in a Zeiss research microscope (Carl Zeiss SMT, Germany) and photographed using a Retiga 2000R Fast digital camera (QImaging, Surrey, BC, Canada) to demonstrate crystallinity.

Scanning Electron Microscopy. Film pieces were plunged into liquid nitrogen and fractured with a prechilled, single-edged razor blade held in a vise-grip locking pliers. The freshly fractured film pieces were retrieved from the liquid nitrogen bath and placed as quickly as possible into a Petri dish containing a piece of filter paper, which was then placed in a desiccator to warm and dry to room temperature. Fractured film pieces were then mounted fractured surface up on a half-stub attached to a full stub using carbon tabs. The samples were then coated with gold−palladium in a Denton Desk II sputter-coating unit (Denton Vacuum U.S.A., Moorestown, NJ). All samples were viewed and photographed in a Hitachi S-4700 field emission scanning electron microscope (Hitachi, Japan) at 2 kV.

Water Vapor Permeability. The gravimetric modified cup method (*15*), based on ASTM E96-80, was used to determine WVP. A single sheet of film was sealed to the test cup (polymethylmethacrylate or Plexiglas) base with a ring containing a 19.6 cm^2 opening using four screws symmetrically located around the cup circumference. Deionized water was placed in the bottom of the test cup to expose the film to high water activity inside the test cups. The films in the cup were oriented with the shiny side (the film side originally in contact with the Mylar cover) facing down (toward the inner, high relative humidity (RH) environment of the cup) (*16*). Average stagnant air gap heights between the water and the film were 70 mm. Eight test cups containing the same film were inserted into a testing cabinet, which had been equilibrated to 0% RH using calcium sulfate desiccant. The cabinet was held at 22.3 ± 0.9 °C using a variable speed controlled fan to maintain constant and uniform temperature and RH, respectively. Each cup was weighed eight times during 24 h using a Mettler Toledo AT460 laboratory-scale balance (d = 0.1 mg/1 mg). The RH at the underside of each film and the corrected WVP were calculated by the WVP correction method (*15*), accounting for the effect of the water vapor concentration gradient through the stagnant air layer in the cups.

Mechanical Property Measurements. After drying, films were cut into test strips of 13 × 100 mm rectangular midsections with 25 × 35 mm gripping ends. At least 16 replicates of each film were tested. The test strips were preconditioned at 33% RH for 72 h using a saturated solution of $MgCl_2$ at 21 °C. Preconditioning before the tensile measurements enables a true comparison of mechanical strength of the films.

Tensile strength (TS) and percentage elongation at break were determined in an Instron Universal Testing Machine (model 1122, Instron Corp., Canton, MA). The instrument was operated with self-alignment hydraulic grips that consist of one fixed and one free end. The free end moves easily into alignment when a load is applied. The gripping ends of the film test strips were clamped, and films were stretched using a speed of 7.5 mm/min using a 100N load cell.

The water content of the preconditioned films at 33% RH was determined using a dynamic vapor sorption analyzer DVS-1 (Surface Measurement Systems, Allentown, PA). Each film was subjected to 33 and 0% RH,

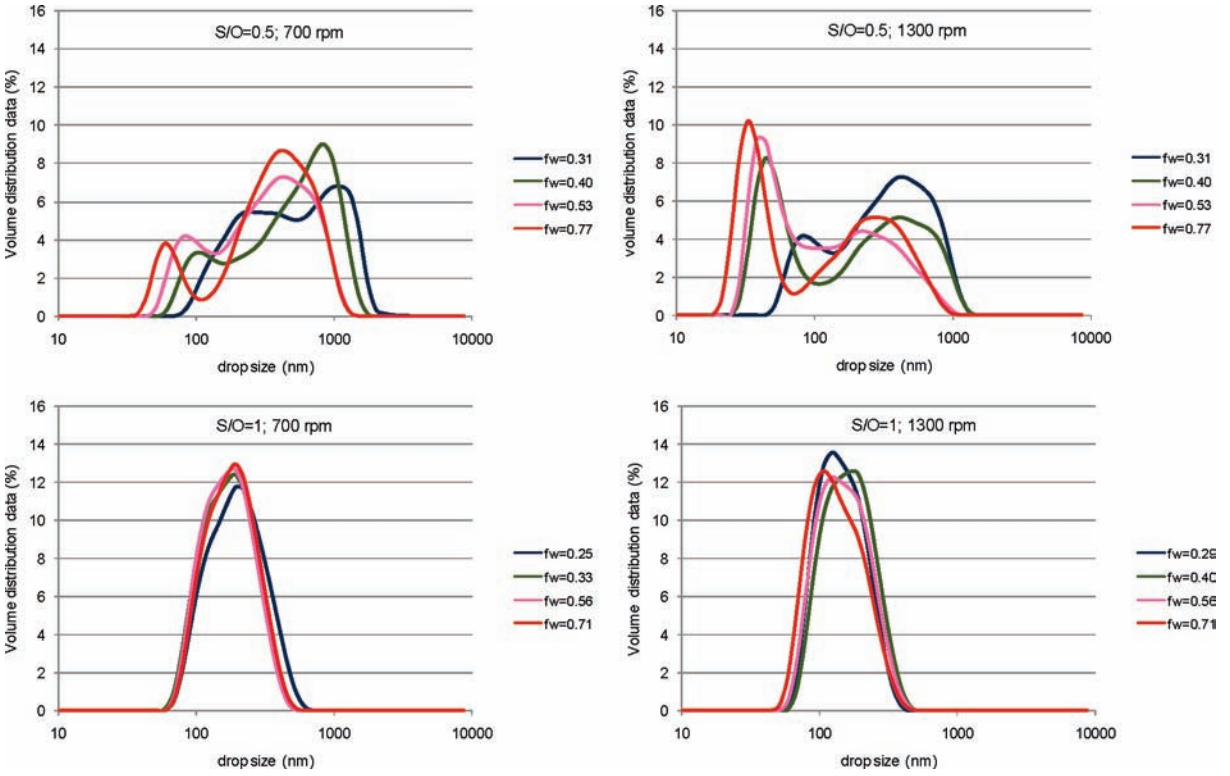

Figure 1. Evolution of droplet size distribution of the inverted Acetem/water emulsion as a function of water fraction (f_w) for two different surfactant-to-oil ratios and agitation speeds. Water addition rate = 1 mL/min.

and the response of the sample was measured gravimetrically over time until the sample reached equilibrium. Three replicates of each film were tested.

RESULTS AND DISCUSSION

CPI Emulsification. The inversion of a water-in-oil to an oil-in-water emulsion was marked by a considerable change in droplet size. **Figure 1** shows the evolution of droplet size distribution (by volume distribution) of the already inverted emulsions as a function of water fraction (f_w) for the different compositions and stirring speeds.

The droplet size distribution varied with surfactant concentration; at a low concentration (S/O = 0.5) a bimodal distribution was observed (**Figure 1**). The position of the two peaks depended on agitation speed; high-speed agitation shifted both peaks to lower diameter values, which can be interpreted in terms of increasing droplet disruption and therefore the volume of droplets with smaller sizes. Increasing surfactant concentration (S/O = 1) resulted in single peaks at about 190 and 120 nm for low and high agitation speeds, respectively. The results suggest that the mechanisms of droplet formation at low surfactant concentration are different from those at high surfactant concentration.

At low surfactant concentration, the droplets with extremely small mean particle diameters (< 100 nm) likely originate due to the formation of multiple droplets. The aqueous phase can entrain internal droplets from the continuous phase through the formation of multiple emulsions O/W/O (*17*−*22*). In fact, the formation of multiple emulsions occurs more frequently in abnormal emulsions in which the favored morphology is not dominant in the external phase. As a result, the favored emulsion is formed in the internal phase and oil can diffuse into inverted micelles and be released into the water upon inversion. The second peak (**Figure 1**) indicates the existence of large oil droplets formed from a continuous oil phase that was trapped between coalescing water droplets at the final catastrophic inversion point.

At a high concentration of surfactant, water droplets show more tendencies for inclusion (*6*, *18*, *23*). Oil droplets are primarily emulsified inside the water droplets via internal phase emulsification, and the increase in oil volume fraction inside the water droplets likely results in droplet coalescence, releasing oil droplets into the water continuous phase larger than those found at lower surfactant concentrations.

At high surfactant concentration, the value of f_w required for inversion depended on agitation intensity during the mixing process. The inversion moved to a highly dispersed phase fraction as stirrer speed increased, in agreement with the findings of others (*24*, *25*). The difference between the breaking and coalescing rates of the oil droplets may be the controlling factor that determined the inversion point. Thus, a higher water fraction is required to offset the increase in droplet disruption caused by an increase in stirring speed. The phase inversion point was also affected by surfactant concentration. At higher surfactant concentration, phase inversion occurs at lower f_w. This is likely related to the fact that the extent of inclusion increased with surfactant concentration. A more extensive inclusion, triggered by the presence of a large amount of surfactant in the water phase, can hasten the inversion to O/W morphology because a larger volume of oil drops inside the water drops will increase the water drop volume until the critical dispersed phase packing is achieved; at this point, phase inversion occurs.

Evolution of Droplet Size with Emulsification Time. The variation in oil droplet size with emulsification time, or droplet size evolution, was determined using data from a particle size analyzer, where *z*-average and PDI were collected. **Figure 2** shows the effect of stirrer speed and emulsifier concentration on droplet size of the inverted O/W emulsion over 360 min. As expected, the droplet size decreased as mixing rate increased due to the greater mechanical energy provided by the impeller, which caused the droplets to break apart. Surfactant concentration also affected

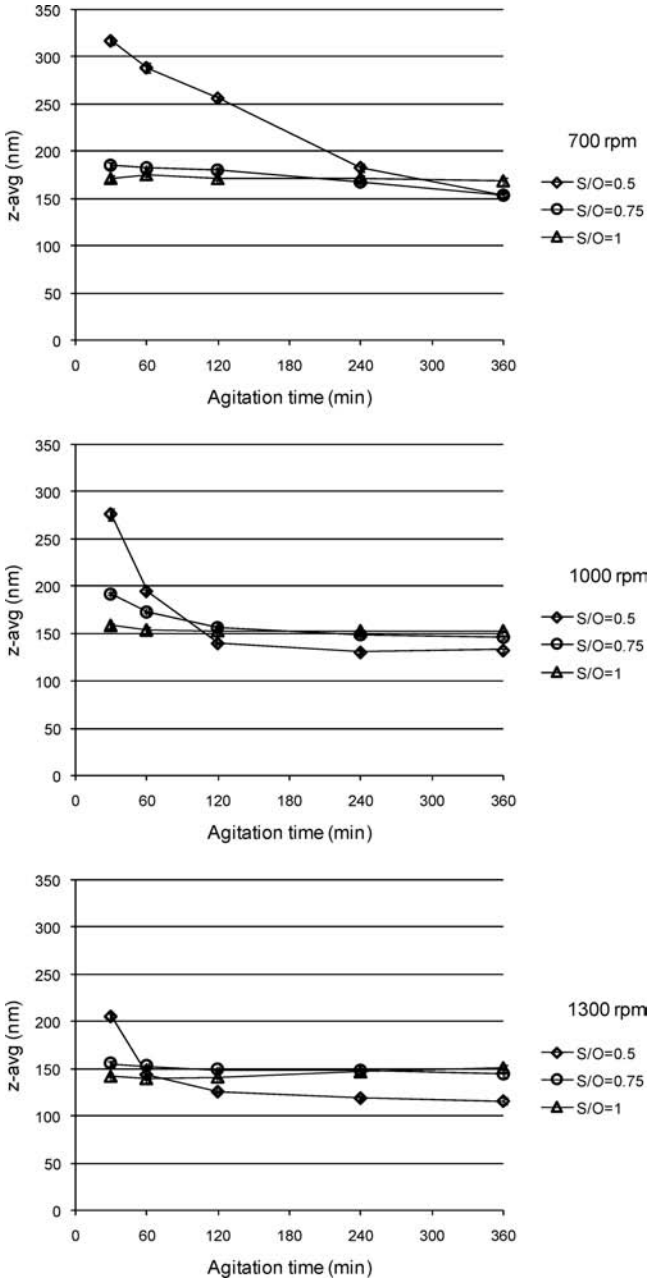

Figure 2. Comparison of *z*-average values of the inverted Acetem/water emulsions containing different surfactant-to-oil ratios during emulsification time at different agitation speeds.

the droplet size of the emulsion. It is known that the addition of a large amount of surfactant to conventional emulsions will result in significant reductions of the oil droplets. According to **Figure 2**, at the beginning of the emulsification process, the emulsion droplet size was found to decrease with increasing surfactant concentration, which was attributed to the increase in interfacial area and the decrease in interfacial tension. However, over time, the trend was reversed. In fact, at the end of the emulsification process, the finest emulsions were those formed at the lowest surfactant concentrations. Droplets formed under low surfactant concentration were quite stable, and the prolonged agitation reduced droplet size considerably in the resulting inverted O/W emulsion. However, at high surfactant concentration, further mixing at 1300 rpm led to a slight increase in droplet size. The main mechanism for destabilization of nanoemulsions is often attributed to Ostwald ripening, when, in this instance, larger

Table 2. Polydispersity Index (PDI) of the Acetem/Water/Tween 60 Emulsions

		agitation time	
agitation speed (rpm)	S/O[a] ratio	30 min	360 min
700	0.5	0.218 ± 0.010 c	0.196 ± 0.019 c
	0.75	0.166 ± 0.011 b	0.192 ± 0.013 b
	1	0.128 ± 0.010 a	0.142 ± 0.012 a
1000	0.5	0.241 ± 0.013 c	0.184 ± 0.008 b
	0.75	0.190 ± 0.009 b	0.170 ± 0.009 b
	1	0.132 ± 0.011 a	0.135 ± 0.008 a
1300	0.5	0.234 ± 0.007 c	0.252 ± 0.028 c
	0.75	0.175 ± 0.019 b	0.177 ± 0.014 b
	1	0.128 ± 0.018 a	0.154 ± 0.012 a

[a] S/O, surfactant/oil.

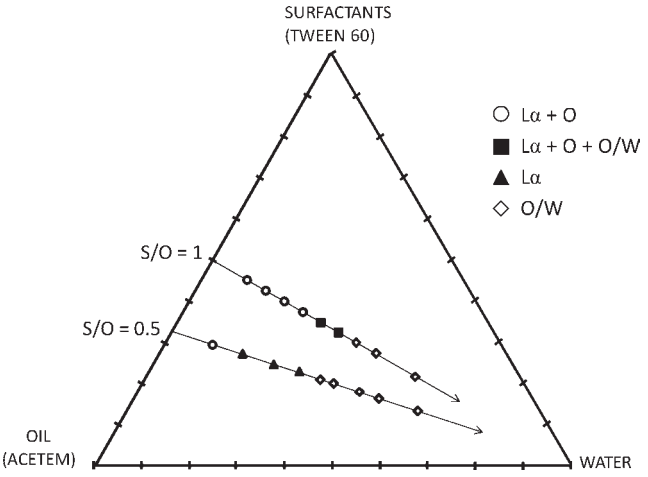

Figure 3. Equilibrium phases of the system Acetem/water/Tween 60.

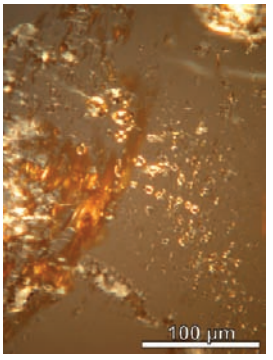

Figure 4. Polarizing optical photomicrograph of Acetem/water/Tween 60 showing a pure lamellar liquid crystalline phase.

droplets grow in size at the expense of smaller droplets due to molecular diffusion of the oil through the continuous phase. Some authors have found that the droplets generally grow more rapidly in emulsions containing higher surfactant concentrations (*26*, *27*).

Table 2 shows the PDI values obtained. PDI values were not significantly affected by agitation time or speed at the 95% confidence interval. However, PDI values decreased significantly as surfactant content increased.

Phase Diagram. Small droplet nanoemulsions can be obtained through CPI emulsification if all of the components are solubilized in a single phase (bicontinuous microemulsion or lamellar

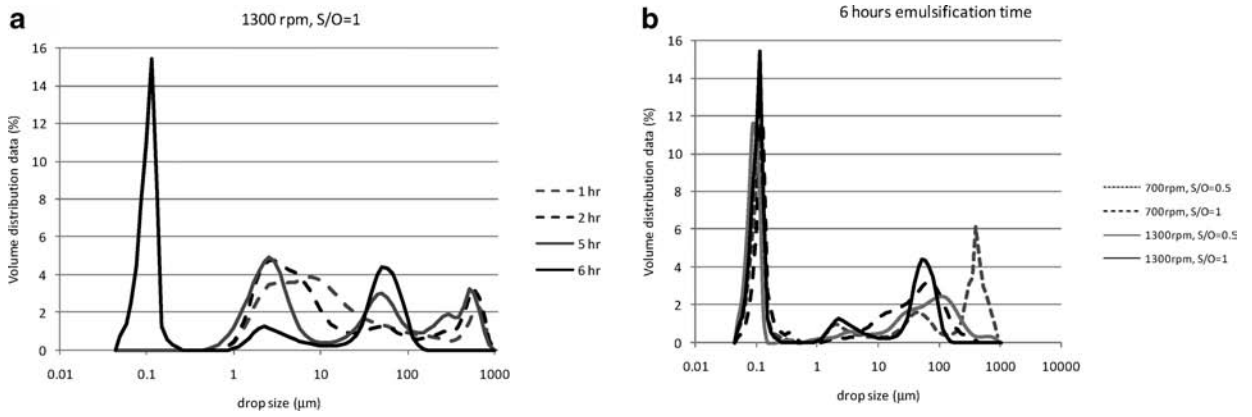

Figure 5. Droplet size distribution obtained by direct emulsification: (**a**) effect of emulsification time; (**b**) effect of surfactant concentration and agitation speed.

liquid crystal) during the emulsification process (*27*, *28*). Therefore, the equilibrium phases present during the dilution of fixed S/O ratio samples were studied. The resulting emulsions were examined in a light microscope through crossed polarizing filters to identify the presence of lamellar liquid crystalline phases indicated by the presence of birefringence. **Figure 3** shows the phase diagram for 1300 rpm agitation speed. At low surfactant concentration, the phases crossed along the emulsification path have the oil component totally solubilized at 18% water content; therefore, a region of pure lamellar liquid crystals is observed from 18 to 31% water content (**Figure 4**). Phase inversion occurs at water contents above 31%, and the oil, which is incorporated into the system, is then redistributed, forming a single O/W phase. However, at high surfactant concentrations, in the furthest zone from the water corner, a lamellar liquid crystalline phase (Lα) coexists with an excess oil phase (O) for a water concentration of up to approximately 25%. Phase inversion begins between 25 and 29% water, forming an oil-in-water (O/W) phase that coexists with the crystalline and excess oil phases for water concentrations up to 33%. Above 33% water, a single oil-in-water phase exists. The different phases in a single sample are indicative of the emulsification stages at various locations of the sample. As water was added to oil during the emulsification process, a high concentration of surfactant provoked a large increase in sample viscosity, which could have shifted the flow from turbulent to laminar. The flow appeared to be laminar around and stagnant away from the impeller. Thus, catastrophic emulsification first occurred closest to the impeller and the rest of the sample as the oil was incorporated into the crystalline region and the crystalline region was diluted with water.

Comparison with Direct Emulsification. Figure 5a shows the evolution in droplet size distribution during 6 h of emulsification at high stirring speed (1300 rpm) and at high surfactant concentration (S/O = 1). When emulsions were prepared by direct emulsification, droplet sizes on the order of 100 nm were achieved after 6 h of continuous agitation instead of the 30 min needed when emulsions were prepared by CPI emulsification (**Figure 1**). When using CPI emulsification, the small droplet size is mainly due to the internal emulsification of the continuous phase inside the droplets of the disperse phase; however, when using direct emulsification, the droplet size is due to the difference between droplet coalescence and droplet disruption rate, increasing 12 times the time needed to achieve droplet sizes of around 100 nm. **Figure 5b** shows that an increase in agitation speed or in surfactant concentration decreased the size of the larger droplets of the emulsion. However, under all conditions studied relatively large droplets of around 100 μm formed when emulsions were prepared by direct emulsification.

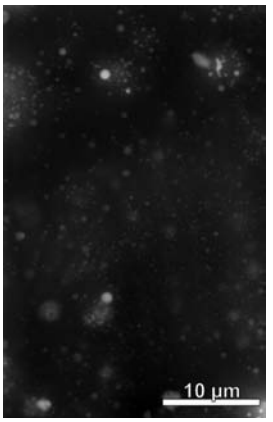

Figure 6. SEM micrograph of emulsion containing cinnamon oil in Acetem prepared by catastrophic phase inversion emulsification.

Films Containing Essential Oils. Essential oils were mixed with Acetem to produce emulsions by CPI emulsification with the presence of oregano oil or cinnamon oil. Attempts to obtain spontaneous emulsification by using oregano oil or cinnamon oil without Acetem were unsuccessful and resulted in broken emulsions or phase separation. However, the solubility of the essential oils in Acetem enhanced the solubility of the essential oils in oil-in-water, and emulsions were formed by CPI. **Figure 6** shows a SEM image of the emulsion containing cinnamon oil. The *z*-average and PDI of the emulsion containing oregano oil were 362 nm and 0.32, respectively, whereas the values for the emulsion containing cinnamon oil were 306 nm and 0.44, respectively.

The essential oil emulsions were incorporated into soy protein-based film-forming solutions to cast edible films. Because of their small sizes, droplet coalescence was avoided, achieving sufficient short-term stability to minimize creaming during film drying. When coalescence was not prevented by reducing the oil droplet size, oil droplets fused and formed large oil droplets on the film surface.

Table 3 shows the mechanical properties and WVP of the soy protein-based films. Films containing oregano oil or cinnamon oil had comparable mechanical properties. Both films showed higher strength values compared to the Acetem and control films, which could be due to the lower water content of the essential oil containing films (**Table 3**). Similar results were found by Atares et al. (*29*) when adding cinnamon oil to ISPi films. The presence of essential oils in the films acting as plasticizers could increase the values of the elongation compared to the control and Acetem films, although this increase was not significantly different. Water barrier properties improved with the addition of Acetem and oregano oil due to an increased concentration of lipids in the

Table 3. Water Vapor Permeability and Mechanical Properties of Isolated Soy Protein-Based Films[a]

film[b]	tensile strength at break (kPa)	elongation at break (%)	Young's modulus (kPa/mm)	x_w (wb) at 33% RH (%)	% RH at film underside	WVP (g·mm/kPa·h·m^2)
ISP	2183 ± 147 a	73 ± 20 NS	1302 ± 58 b	5.26 ± 0.08	84 ± 1 NS	1.54 ± 0.06 b
AC/ISP	2258 ± 296 a	74 ± 17	1116 ± 88 a	4.96 ± 0.11	88 ± 1	1.21 ± 0.08 a
OR/AC/ISP	3204 ± 478 b	87 ± 14	1216 ± 90 b	3.82 ± 0.76	86 ± 1	1.24 ± 0.11 a
CN/AC/ISP	3256 ± 326 b	84 ± 19	1314 ± 90 b	3.81 ± 0.33	85 ± 2	1.64 ± 0.10 b

[a] Different letters indicate significant differences at 95% confidence level. NS, no significant difference. [b] ISP, isolated soy protein; AC, Acetem; OR, oregano oil; CN, cinnamon oil.

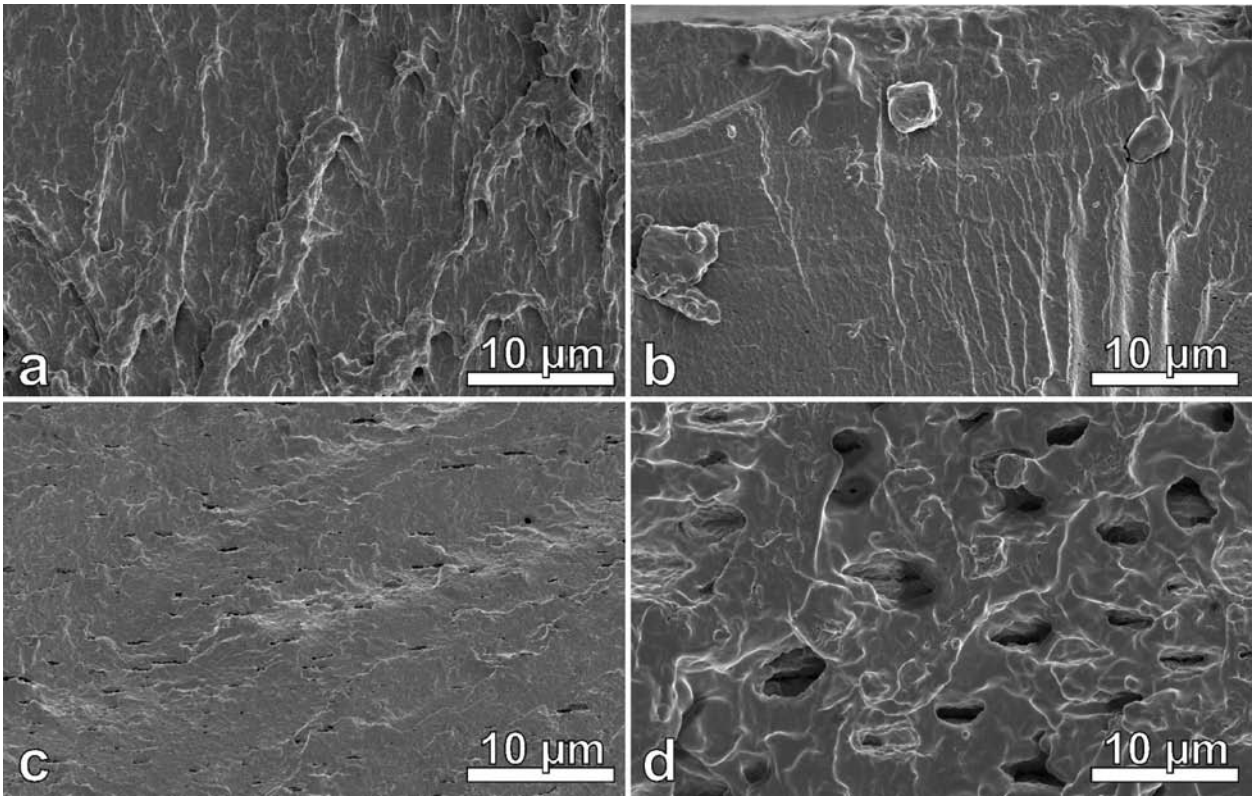

Figure 7. Cross-sectional surfaces of ISP-based films: (**a**) ISP; (**b**) ISP/Acetem; (**c**) ISP/Acetem/oregano oil; (**d**) ISP/Acetem/cinnamon oil.

protein films. However, addition of cinnamon oil increased the permeability values to levels similar to those of the control film. This result was attributed to an increase in the water vapor diffusivity through the film containing cinnamon oil because the cross section of this film showed a more porous matrix (**Figure 7d**) compared to the other films.

Conclusions. When using the system Acetem/water/Tween 60, CPI emulsification produced finer emulsions than direct emulsification. The Acetem/water/Tween 60 emulsions when prepared by CPI emulsification produced nanoemulsions having mean particle diameter and polydispersity between 115 and 170 nm and between 0.14 and 0.20, respectively. The *z*-average and droplet size distribution during CPI depended on stirring speed and surfactant concentration. The finest and most stable emulsions were obtained when low surfactant concentration at high stirring speed was used. This behavior can be explained through the phases crossed along the emulsification paths. The crossing of a liquid crystalline phase along the emulsification path through the phase diagram was shown to be important as was remaining in this region long enough to allow proper mixing throughout the entire sample.

Acetem also proved to be a useful carrier for essential oils; nanoemulsions containing oregano oil or cinnamon oil were prepared by CPI emulsification. The resulting composite films composed of a continuous soy protein matrix with lipidic globules containing oregano oil had better mechanical and WVP properties than the ISP films.

LITERATURE CITED

(1) Garti, N.; Aserin, A. Chapter 19: Nanoscale liquid self-assembled dispersions in foods and the delivery of functional ingredients. In *Understanding and Controlling the Microstructure of Complex Foods*; McClements, D. J., Ed.; Woodhead Publishing: Cambridge, U.K., 2007; pp504−553.

(2) Chen, H.; Weiss, J.; Shahidi, F. Nanotechnology in nutraceuticals and functional foods. *Food Technol.* **2006**, *60* (3), 30−36.

(3) Schubert, H.; Ax, K. Engineering food emulsions. In *Part II: Product Development*; Woodhead Publishing: Cambridge, U.K., 2003; Chapter 8.

(4) Weiss, J.; Takhistov, P.; McClements, J. Functional materials in food nanotechnology. *J. Food Sci.* **2006**, *71* (9), R107−R116.

(5) Ochomogo, M.; Monsalve-Gonzalez, A. *Natural flavor enhancement compositions for food emulsions*. U.S. Patent Appl. 20090196972; Clorox Co., Oakland, CA.

(6) Jahanzad, F.; Crombie, G.; Innes, R.; Sajjadi, S. Catastrophic phase inversion via formation of multiple emulsions: a prerequisite for formation of fine emulsions. *Chem. Eng. Res. Des.* **2009**, *87* (4), 492−498.

(7) Shinoda, K.; Saito, H. The stability of O/W type emulsions as functions of temperature and the HLB of emulsifiers: the emulsification by PIT-method. *J. Colloid Interface Sci.* **1969**, *26* (1), 70−74.
(8) Constantinides, P. P.; Yiv, S. H. Particle size determination of phase-inverted water in oil microemulsions under different dilution and storage conditions. *Int. J. Pharm.* **1995**, *115* (2), 225−234.
(9) Thakur, R. K.; Villete, C.; Aubry, J. M.; Delaplace, G. Formulation−composition map of lecithin-based emulsion. *Colloids Surf., A* **2007**, *310* (1−3), 55−61.
(10) Solans, C.; Izquierdo, P.; Nolla, J.; Azemar, N.; Garcia-Celma, M. J. Nano-emulsions. *Curr. Opin. Colloid Interface Sci.* **2005**, *10* (3−4), 102−110.
(11) Sajjadi, S.; Jahanzad, F.; Yianneskis, M. Catastrophic phase inversion of abnormal emulsions in the vicinity of the locus of transitional inversion. *Colloids Surf., A* **2004**, *240* (1−3), 149−155.
(12) Sajjadi, S. Effect of mixing protocol on formation of fine emulsions. *Chem. Eng. Sci.* **2006**, *61* (9), 3009−3017.
(13) Porras, M.; Martinez, A.; Solans, C.; Gonzalez, C.; Gutierrez, J. M. Ceramic particles obtained using W/O nano-emulsions as reaction media. *Colloids Surf., A* **2005**, *270−271*, 189−194.
(14) Guilbert, S. Technology and application of edible protective films. In Mathlouthi, M., Ed., *Food Packaging and Preservation*; Elsevier Applied Science Publisher: New York, 1986; pp 371−394.
(15) McHugh, T. H.; Avena-Bustillos, R.; Krochta, J. M. Hydrophilic edible films: modified procedure for water vapor permeability and explanation of thickness effects. *J. Food Sci.* **1993**, *58* (4), 899−903.
(16) Avena-Bustillos, R.; Krochta, J. M. Water vapor permeability of caseinate-based films as affected by pH, calcium crosslinking and lipid content. *J. Food Sci.* **1993**, *58* (4), 904−907.
(17) Greiner, R. W.; Evans, D. F. Spontaneous formation of a water-continuous emulsion from a W/O microemulsion. *Langmuir* **1990**, *6* (12), 1793−1796.
(18) Sajjadi, S.; Zerfa, M.; Brooks, B. W. Dynamic behavior of droplets in oil/water/oil dispersions. *Chem. Eng. Sci.* **2002**, *57* (4), 663−675.
(19) Brooks, B. W.; Richmond, H. N. Dynamics of liquid−liquid phase inversion using non-ionic surfactants. *Colloids Surf.* **1991**, *58* (1−2), 131−148.
(20) Morais, J. M.; Santos, O. D. H.; Nunes, J. R. L.; Zanatta, C. F.; Rocha-Filho, P. A. W/O/W multiple emulsions obtained by one-step emulsification method and evaluation of the involved variables. *J. Dispersion Sci. Technol.* **2008**, *29* (1), 63−69.
(21) Xie, F.; Brooks, B. W. Phase behavior of a non-ionic surfactant-polymeric solution-water system during the phase inversion process. *Colloids Surf., A* **2005**, *252* (1), 27−32.
(22) Zerfa, M.; Sajjadi, S.; Brooks, B. W. Phase behavior of polymer emulsions during phase inversion process in the presence of non-ionic surfactants. *Colloids Surf., A* **2001**, *178* (1−2), 41−48.
(23) Sajjadi, S.; Jahanzad, F.; Brooks, B. W. Phase inversion in abnormal o/w/o emulsions: I. Effect of surfactant concentration. *Ind. Eng. Chem. Res.* **2002**, *41* (24), 6033−6041.
(24) Brooks, B. W.; Richmond, H. N. Phase inversion in non-ionic surfactant-oil-water systems-II. Droplet size studies in catastrophic inversion with turbulent mixing. *Chem. Eng. Sci.* **1994**, *49* (7), 1065−1075.
(25) Quinn, J. A.; Sigloh, D. B. Phase inversion in the mixing of immiscible liquids. *Can. J. Chem. Eng.* **1963**, *41*, 15−18.
(26) Ee, S. L.; Duan, X; Liew, J.; Nguyen, Q. D. Dropletlet size and stability of nano-emulsions produced by the temperature phase inversion method. *Chem. Eng. J.* **2008**, *140* (1−3), 626−631.
(27) Izquierdo, P.; Esquema, J.; Tadros, Th. F.; Dederen, C.; Garcia, M. J.; Azemar, N.; Solans, C. Formation and stability of nano-emulsions prepared using the phase inversion temperature method. *Langmuir* **2002**, *18* (1), 26−30.
(28) Morales, D.; Gutiérrez, J. M.; García-Celma, M. J.; Solans, C. A study of the relation between bicontinuous microemulsions and oil/water nano-emulsion formation. *Langmuir* **2003**, *19* (18), 7196−7200.
(29) Atarés, L.; de Jesús, C.; Talens, P.; Chiralt, A. Characterization of SPI-based edible films incorporated with cinnamon or ginger essential oils. *J. Food Eng.* **2010**, *99* (3), 384−391.

Received for review June 17, 2010. Revised manuscript received September 30, 2010. Accepted October 4, 2010.